Two-Phase Nanofluid Thermal Analysis over a Stretching Infinite Solar Plate Using Keller Box Method (KBM)

Mosayebidorcheh, Sobhan* [+]
Young Researchers and Elite Club, Najafabad Branch, Islamic Azad University, Najafabad, I.R. IRAN

Vatani, Mahshid
Department of Mechanical Engineering, Babol University of Technology, Babol, I.R. IRAN

Hatami, Mohammad [•]
Department of Mechanical Engineering, Esfarayen University of Technology, Esfarayen, North Khorasan, I.R. IRAN

Domiri Ganji, Davood
Department of Mechanical Engineering, Babol University of Technology, Babol, I.R. IRAN

ABSTRACT: *In the present study, two phase nanofluid flow in a three dimensional system is modeled over a stretching infinite solar plate and the heat transfer analysis is performed for this problem. The governing equations are presented based on previous studies and the suitable solution method is recommended due to infinite boundary condition in the problem. Keller Box Method (KBM) using the Maple 15.0 mathematical software is applied as the solution method for the governing equation of the problem. The effect of some parameters existed in the equations (Pr (Prandtl number), Sc (Schmidt number), Nb (Brownian motion parameter), Nt (Thermophoresis parameter), λ=b/a (ratio of the stretching rate along y to x directions) and n (power-law index)), are discussed on the velocities, temperature, and nanoparticles concentration functions. As an important outcome, increasing both n and λ parameters, makes a reduction in shear stress, while it increase the Nusselt number function of heat transfer.*

KEYWORDS: *Solar plate; Nanofluid; Nanoparticle concentration; Infinite boundary; Keller Box Method (KBM).*

INTRODUCTION

Due to high efficiency, clean energy and low costs of solar energy, it is widely investigated by the researchers to improve its performance such as using the nanofluids to increase the thermal efficiency of the solar devises [1].

***** *To whom correspondence should be addressed.*
\+ *E-mail: sobhanmosayebi@yahoo.com*
• *Other Address: International Research Center for Renewable Energy, State Key Laboratory of Multiphase Flow in Power Engineering, Xi'an Jiaotong University, Xi'an 710049, P.R. China*
1021-9986/2018/6/247-256 10/$/6.00

Recently *Gorji* and *Ranjbar* [2] evaluated the effect of varying geometry on the overall thermal performance a nanofluid based Direct Absorption Solar Collector (DASC). They used Box–Behnken design and response surface methodology to study and optimize the main and interaction effects of the dimensions on the system overall thermal performance. Although they considered rectangular shape for the solar collector, *Nasrin* and *Alim* [3] investigated the thermal performance for a wavy solar collector filled by nanofluids numerically. Except for experimental and numerical works in this field, some researchers worked analytically on the nanofluids treatment in solar applications. *Ahmad Khan et al.* [4] analyzed the three-dimensional flow of nanofluid over an elastic sheet stretched non-linearly in two lateral directions under the solar radiation using the Runge-Kutta method. In another analytical study, *Cregan* and *Myers* [5] considered a system of two differential equations; a radiative transport equation describing the propagation of solar radiation through the nanofluid and an energy equation for the steady state, two-dimensional model of an inclined nanofluid-based direct absorption solar collector. *Turkyilmazoglu* [6] evaluated the alumina nanoparticles effect on the thermal performance of a water based solar collector analytically. The solution of the particle's motion in different fluids media has been considered by the authors widely [7-10].

Comparison of the single and two-phase modeling for the nanofluids has been considered by the researchers. For instance, Haghshenas *Fard et al.* [11] compared the results of the single phase and two-phase numerical methods for nanofluids in a circular tube. They reported that for Cu-water the average relative error between experimental data and CFD results based on single-phase model was 16% while for the two-phase model was 8%. In another numerical study, *Göktepe et al*. [12] compared these two models for nanofluid convection at the entrance of a uniformly heated tube which found the same results and confirms the accuracy of two-phase modeling. *Mohyud-Din et al*. [13] in an analytical study, considered the three dimensional heat and mass transfer with magnetic effects for the flow of a nanofluid between two parallel plates in a rotating system. As one of their main outcomes, thermophoresis and Brownian motion parameters are directly related to heat transfer but are inversely related to the concentration profile. Also, they found that higher Coriolis forces decrease the temperature boundary layer thickness. The three-dimensional flow of nanofluids under the radiation (due to solar or etc.) has been analyzed by *Hayat et al.* [14] and *Khan et al.* [15]. They also computed and examined the effects of different parameters on the velocity, temperature, skin friction coefficient and Nusselt number of the nanofluid flow. Other works of nanofluids flow and heat transfer analysis can be found in [16-31].

In this study, it is aimed to investigate the heat transfer and fluid flow of nanofluids on a 3D solar infinite plate by numerical solution of the nonlinear governing equation. To investigate the heat transfer from this plate, the effects of appeared parameters in equations on Nusselt number, temperature profiles, and nanoparticles concentrations are discussed.

PROBLEM DESCRIPTION

A nanofluid flow over a solar plate as proposed by *Khan et al.* [4] is shown in Fig. 1. The flow is incompressible and induced due to plate stretched in two directions by nonlinear functions. The plate is maintained at constant temperature and the mass flux of the nanoparticles at the wall is assumed to be zero. Three-dimensional governing equations will be [4]:

$$\frac{\partial u}{\partial x}+\frac{\partial v}{\partial y}+\frac{\partial w}{\partial z}=0 \tag{1}$$

$$u\frac{\partial u}{\partial x}+v\frac{\partial u}{\partial y}+w\frac{\partial u}{\partial z}=\upsilon_f\,\frac{\partial^2 u}{\partial z^2} \tag{2}$$

$$u\frac{\partial v}{\partial x}+v\frac{\partial v}{\partial y}+w\frac{\partial v}{\partial z}=\upsilon_f\,\frac{\partial^2 v}{\partial z^2} \tag{3}$$

$$u\frac{\partial T}{\partial x}+v\frac{\partial T}{\partial y}+w\frac{\partial T}{\partial z}=\alpha\frac{\partial^2 T}{\partial z^2}+ \tag{4}$$

$$\tau\left[D_B\frac{\partial C}{\partial z}\frac{\partial T}{\partial z}+\frac{D_T}{T_\infty}\left(\frac{\partial T}{\partial z}\right)^2\right]$$

$$u\frac{\partial C}{\partial x}+v\frac{\partial C}{\partial y}+w\frac{\partial C}{\partial z}=D_B\,\frac{\partial^2 C}{\partial z^2}+\left(\frac{D_T}{T_\infty}\right)\frac{\partial^2 T}{\partial z^2} \tag{5}$$

Here *u* and *v* are the velocities in the *x* and *y* directions, respectively, *T* is the temperature, *C* is the concentration, D_B is the Brownian diffusion coefficient

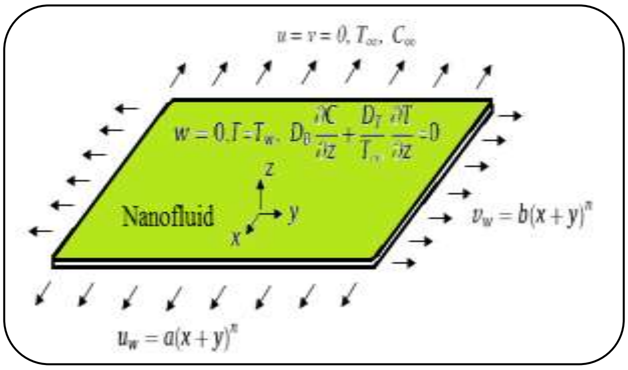

Fig. 1: Schematic of the nanofluid flow over a stretching solar plate.

of the diffusing species and D_T is the thermophoretic diffusion coefficient. Because the plate is infinite and is stretched in two directions by nonlinear functions, the relevant boundary conditions are:

$$u = u_w = a(x+y)^n, v = v_w = b(x+y)^n \tag{6}$$

$$w = 0, T = T_w, D_B \frac{\partial C}{\partial z} + \frac{D_T}{T_\infty}\frac{\partial T}{\partial z} = 0 \quad \text{at} \quad z = 0$$

$$u \to 0, v \to 0, T \to T_\infty, C \to C_\infty \quad \text{as} \quad z \to 0$$

By introducing these parameters:

$$u = a(x+y)^n f'(\eta), v = a(x+y)^n g'(\eta) \tag{7}$$

$$w = -\sqrt{a\upsilon_f}\,(x+y)^{\frac{n-1}{2}}\left(\frac{n+1}{2}(f+g) + \frac{n-1}{2}\eta(f'+g')\right)$$

$$\theta(\eta) = \frac{T - T_\infty}{T_w - T_\infty}, \phi(\eta) = \frac{C - C_\infty}{C_\infty}, \eta = \sqrt{\frac{a}{\upsilon_f}}(x+y)^{\frac{n-1}{2}} z$$

and substituting the above variables into (1)-(5) equations, one can get:

$$f''' + \frac{n+1}{2}(f+g)f'' - n(f'+g')f' = 0 \tag{8}$$

$$g''' + \frac{n+1}{2}(f+g)g'' - n(f'+g')g' = 0 \tag{9}$$

$$\frac{1}{Pr}\theta'' + \frac{n+1}{2}(f+g)\theta' + Nb\phi'\theta' + Nt\theta'^2 = 0 \tag{10}$$

$$\phi'' + \frac{n+1}{2}Sc(f+g)\phi' + \frac{Nt}{Nb}\theta'' = 0 \tag{11}$$

These systems of nonlinear equations should be solved by a powerful numerical or analytical method. In this study OCM is applied with these boundary conditions:

$$f(0) = 0, f'(0) = 1, g(0) = 0, g'(0) = \lambda, \theta(0) = 1, \tag{12}$$

$$Nb\phi'(0) + Nt\theta'(0) = 0$$

$$f'(\infty) \to 0, g'(\infty) \to 0, \theta(\infty) \to 0, \phi(\infty) \to 0$$

where Pr (Prandtl number), Sc (Schmidt number), Nb (Brownian motion parameter), Nt (Thermophoresis parameter), λ=b/a (ratio of the stretching rate along y to x directions) are parameters as defined in [4].

NUMERICAL PROCEDURE

In this study, Keller Box Method (KBM) is used as an efficient numerical method for solving the problem using Maple 15.0 software. The Keller Box scheme is a face-based method for solving partial differential equations that has numerous attractive mathematical and physical properties. It is shown that these attractive properties collectively follow from the fact that the scheme discretizes partial derivatives exactly and only makes approximations in the algebraic constitutive relations appearing in the PDE. The exact Discrete Calculus associated with the Keller-Box scheme is shown to be fundamentally different from all other mimetic (physics capturing) numerical methods. Actually, Keller Box is a variation of the finite volume approach in which unknowns are stored at control volume faces rather than at the more traditional cell centers. The name alludes to the fact that in space-time, the unknowns sit at the corners of the space-time control volume which is a box in one space dimension on a stationary mesh. The original development of the method [32] dealt with parabolic initial value problems such as the unsteady heat equation. The method was made better known by *Cebeci* and *Bradshaw* [33] as a method for the solution of the boundary layer equations.

RESULTS AND DISCUSSIONS

To solve the governing equations of (8)-(11) with boundary conditions in Eq. (12) by numerical methods, the infinite range must be clear. It means that which η can role as the infinite number. To find this value three different numbers (4, 7 and 10) are examined which results are depicted in Fig. 2. As seen for all the profiles (Velocity, Temperature and Nanoparticles concentrations)

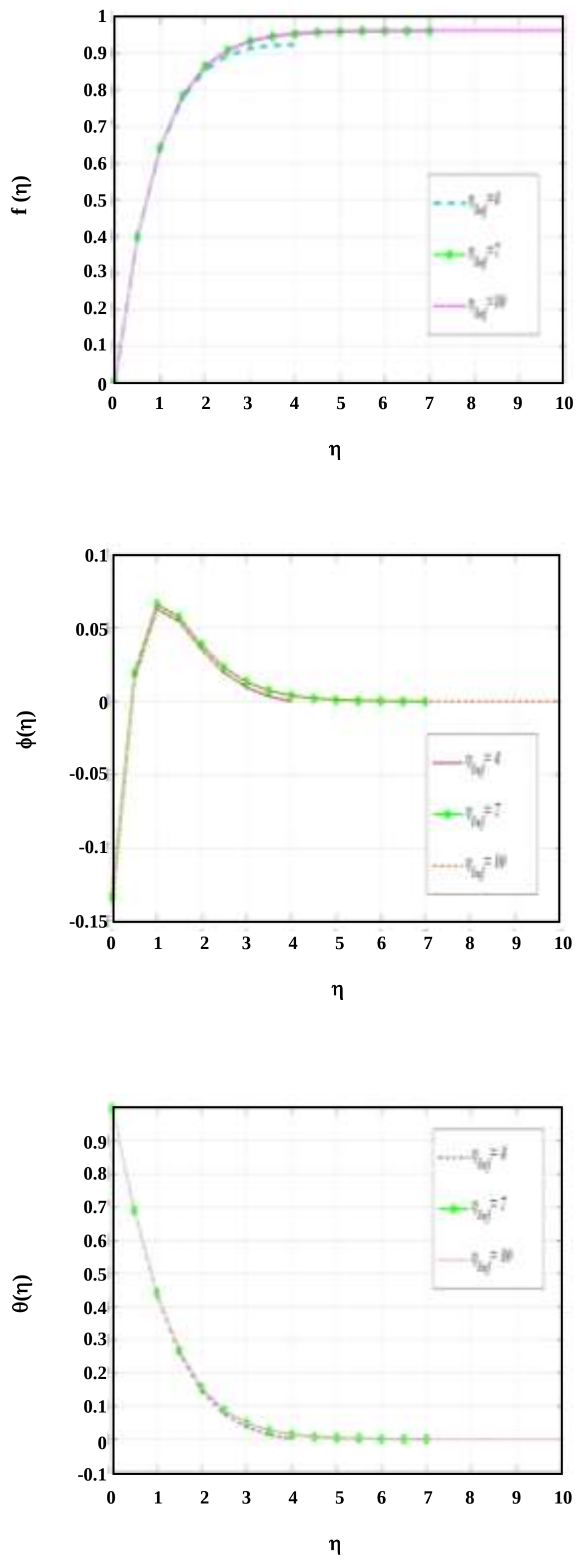

Fig. 2 Effect of η on profiles when n=1, Nb= 0.7, Nt= 0.4, Sc = 2, Pr= 1, λ= 0.5.

the two last values (i.e. 7 and 10) have the same profiles, so increasing this value has not more effect on the results and we choose 7 for it in the solution.

Figs. 3 demonstrate the effect of the power-law index (n) on the x- and y- components of dimensionless velocities ($f'(\eta)$ and $g'(\eta)$ functions) as well as temperature and nanoparticles volume fraction boundary layer profiles ($\theta(\eta)$ and $\varphi(\eta)$). As seen, with the increase of the power-law index n, both the dimensionless velocity in the x- and y-directions decreases, correspondingly. Also, it can be seen that the decrement of velocity in the x-direction and y-direction are equal roughly. Actually, the results show that both velocity profiles are decreasing the function of the power index. Furthermore, it is clear that the thermal boundary layer will be thinner for larger n values while nanoparticles concentration profile become thicker, both of which augments, in turn, the rate of heat transfer from the sheet. It can also be found that the greater the n value is, the faster the decline of θ will be. It is proposed that the increasing n can enhance the convective properties of the fluid since it will increase the deformation by the shear stress from the wall to the fluid.

The effect of Brownian motion parameter (Nb) on the nanoparticles volume fraction function is shown in Fig. 4. This figure reveals that Brownian motion parameter has an inverse effect compared to Nt. Actually, an increase in Nb can lead to a decrease in nanoparticles concentration. Therefore, ϕ will decrease upon the increasing of the Brownian motion parameter Nb. Effect of Schmidt number (Sc) on temperature and nanoparticles volume fraction is shown via Fig. 5.

From the Schmidt number definiation (the ratio of momentum diffusivity to mass diffusivity), an increase in Sc corresponds to the decrease of the Brownian diffusion coefficient D_B. As seen in Fig. 5, the smaller D_B, corresponding to higher Sc numbers, could result in more nanoparticle penetration due to higher momentum diffusivity which in turn gives rise to the shorter penetration depth of nanoparticle volume fraction ϕ.

A higher Prandtl number fluid possesses stronger convection as compared to pure conduction and effective in transferring energy through a unit area. The reduced Nusselt number, therefore, increases with an increase in Pr. Fig. 6 represents the effect of Prandtl number on the

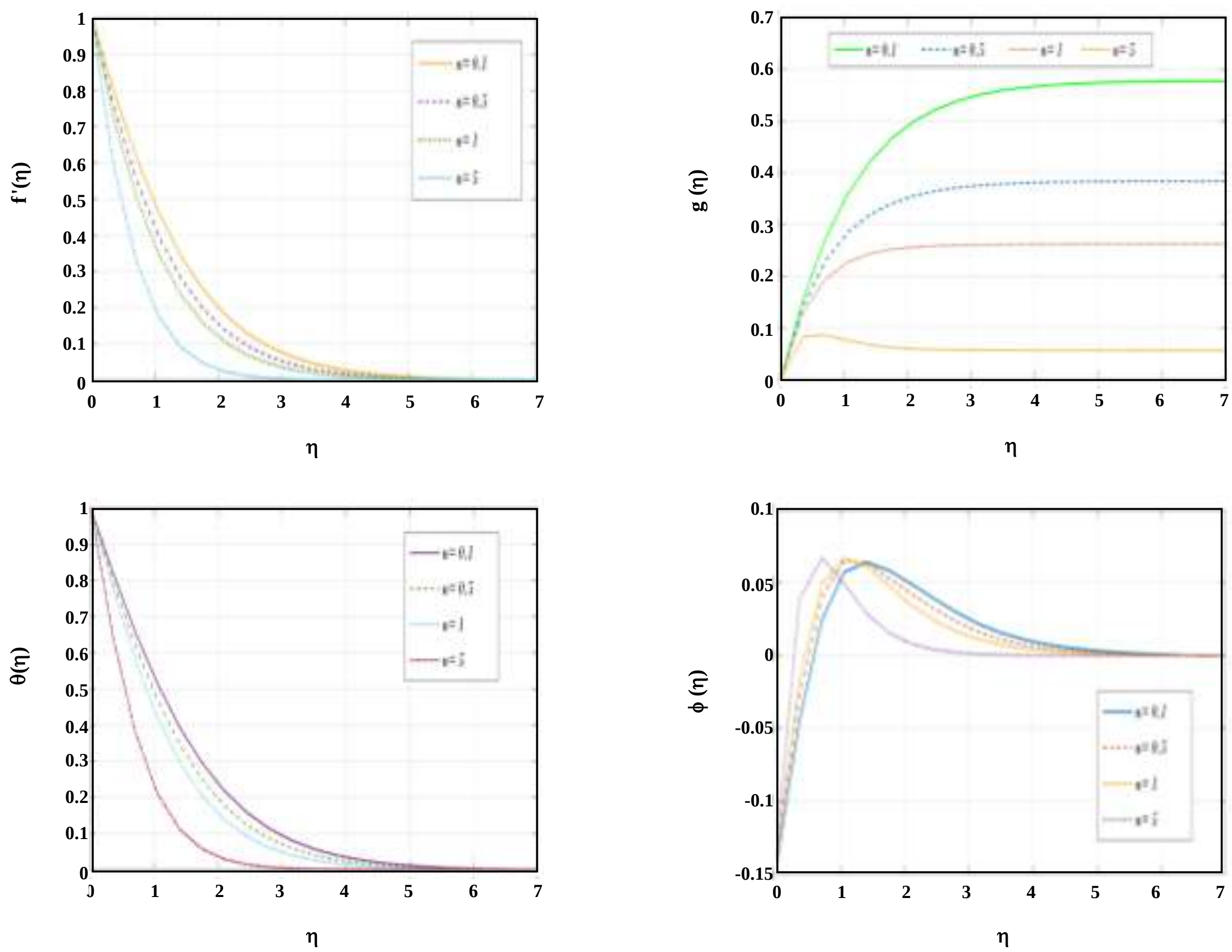

Fig. 3 Effect of power index (n) when η_∞ = 7, Nb= 0.7, Nt = 0.4, Sc= 3, Pr= 1, λ= 0.5.

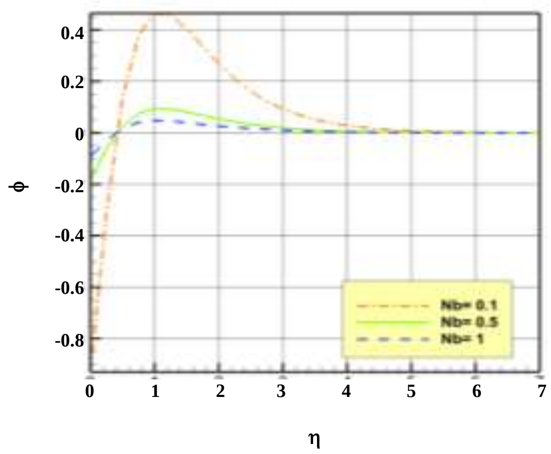

Fig. 4 Effect of Brownian motion parameter (Nb) on nanoparticles volume fraction when η_∞ = 7, n= 1, Nt= 0.4, Sc= 3, Pr= 1, λ= 0.5.

thermal boundary layer. As shown in this figure, temperature θ decreases and becomes very close to the ambient temperature and the slope of temperature distribution near the wall become steeper with an increment of Pr. As *Khan et al.* [4] reported, an increase in Pr accompanies with weaker thermal diffusivity and restricts the heat from flowing deeper into the nanofluid, so thermal boundary layer becomes decreased with an augmentation of Pr.

The influence of stretching rate ratio, λ, on the velocities components and temperature/nanoparticles concentration is presented in Fig. 7. Physically, the increase in stretching rate ratio, or the large values of λ (=b/a), means either increase in b or decrease in a, so it is expected to further lead to an acceleration of the downward flow along the vertical direction, and

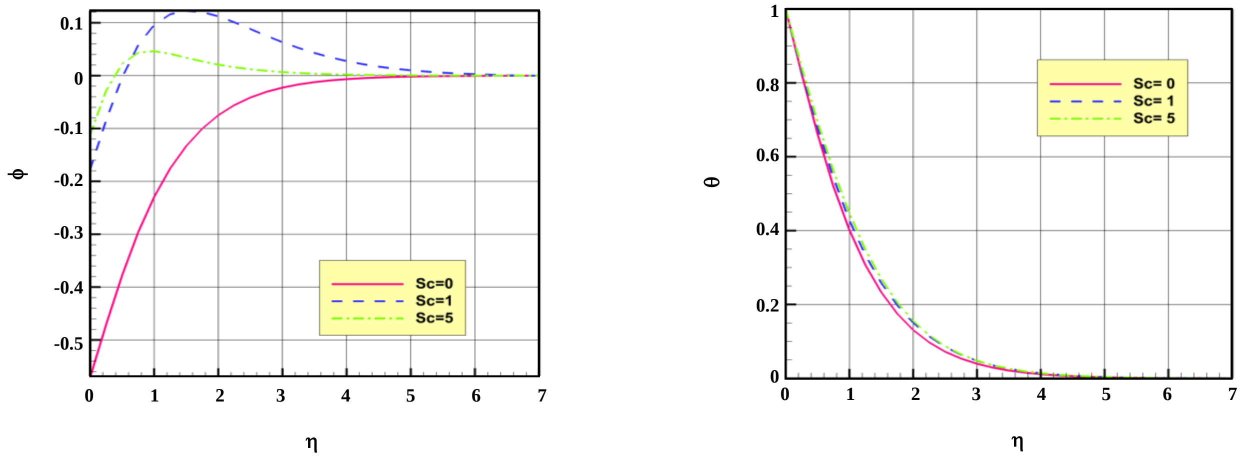

Fig. 5: Effect of Schmidt number (Sc) on temperature and nanoparticles volume fraction when η_∞ = 7, n= 1, Nb= 0.7, Nt = 0.4, Pr= 1, λ= 0.5.

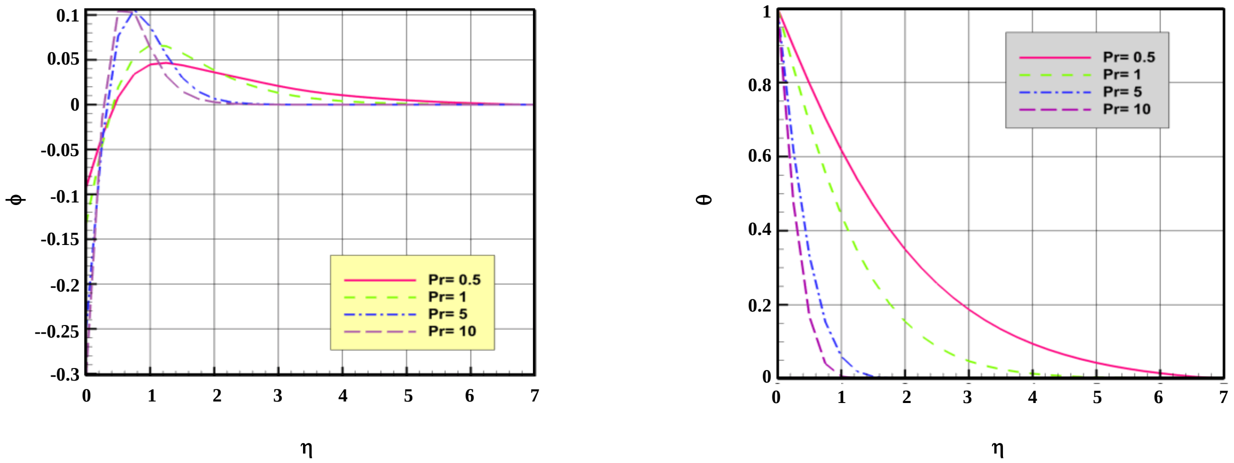

Fig. 6: Effect of Prandtl number (Pr) on temperature and nanoparticles volume fraction when η_∞ = 7, n= 1, Nb= 0.7, Nt = 0.4, Sc= 3, λ= 0.5.

as a result, a decrease in x-component and increase in y-component velocity profiles would occur. Moreover, increasing the stretching rate ratio makes a colder fluid flow due to the higher heat transfer process as can be found in Fig. 7. Consequently, the thermal boundary layer becomes thinner and both temperature and concentration profiles decrease.

The effect of the thermophoretic parameter (Nt) and Prandtl number on the Nusselt number is shown in the 3D contour of Fig. 8. The thermophoretic force is the force that diffuses nanoparticles into the ambient flow and due to the existence of the increased amount of the nanoparticles in the fluid the temperature gradient will be smaller. It is clear that maximum heat transfer occurs when the Nt has minimum and Pr has the maximum values.

Fig. 9 confirms that Sc also has the same effect on Nusselt number, i.e. it makes maximum Nu in the lower values. Finally, the effect of *n* and λ on the shear stress at the surface (i.e., f''(0) and g''(0)) and reduced Nusselt number (Nur) is depicted in Fig. 10. It reveals that increasing both n and λ parameters makes

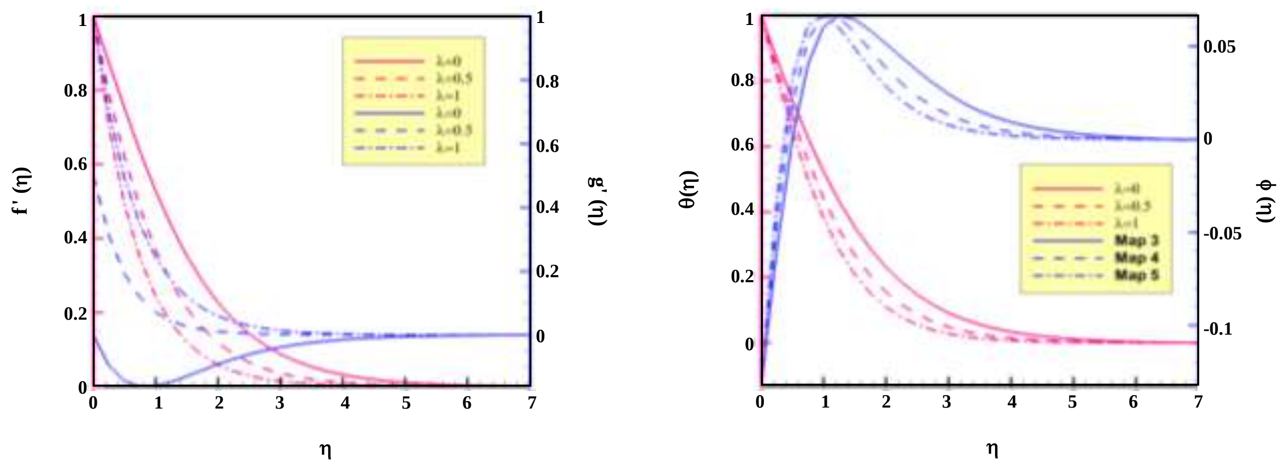

***Fig. 7:** Effect of stretching rate ratio, λ when $\eta_\infty = 7$, n= 1, Nb= 0.7, Nt = 0.4, Sc= 3, λ= 0.5.*

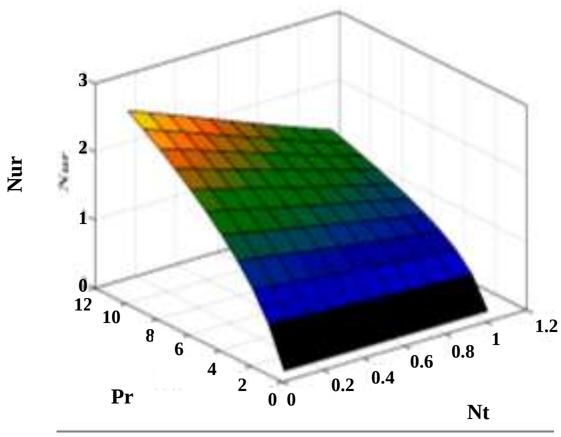

***Fig. 8:** Effect Pr and Nt on the Nur function of when $\eta_\infty = 7$, n= 1, Nb= 0.7, Sc= 3, λ= 0.5.*

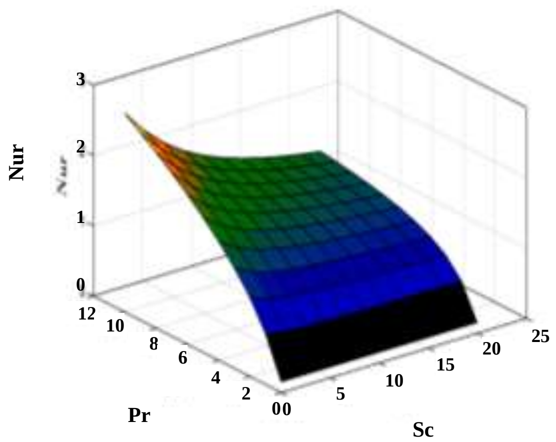

***Fig. 9:** Effect of Pr and Sc on Nur function when $\eta_\infty = 7$, n= 1, Nb= 0.7, Nt= 0.4, λ= 0.5.*

reduction in shear stress, while it increases the Nusselt number function of heat transfer.

CONCLUSIONS

In this study, Keller Box Method (KBM) as a numerical method by Maple 15.0 was applied to find the solution of 3D modeling of heat transfer for two-phase nanofluids flow over an infinite stretching solar plate. Due to infinite boundary condition, it is tried to find the suitable definable value as the infinite in boundary conditions. Comparison results show that 7 is a suitable number for this geometry. As an important outcome from the heat transfer view point, maximum heat transfer occurs when the thermophoretic parameter (Nt) has minimum and Prandtl (Pr) has the maximum values. Also, increasing both power index (n) and λ parameters, makes a reduction in shear stress, while increases the Nusselt number.

Acknowledgments

The authors gratefully acknowledge the financial support of the National Natural Science Foundation of China (No. 51422604, 21276206) and the National 863 Program of China (No. 2013AA050402).This work was also supported by the China Fundamental Research Funds for the Central Universities.

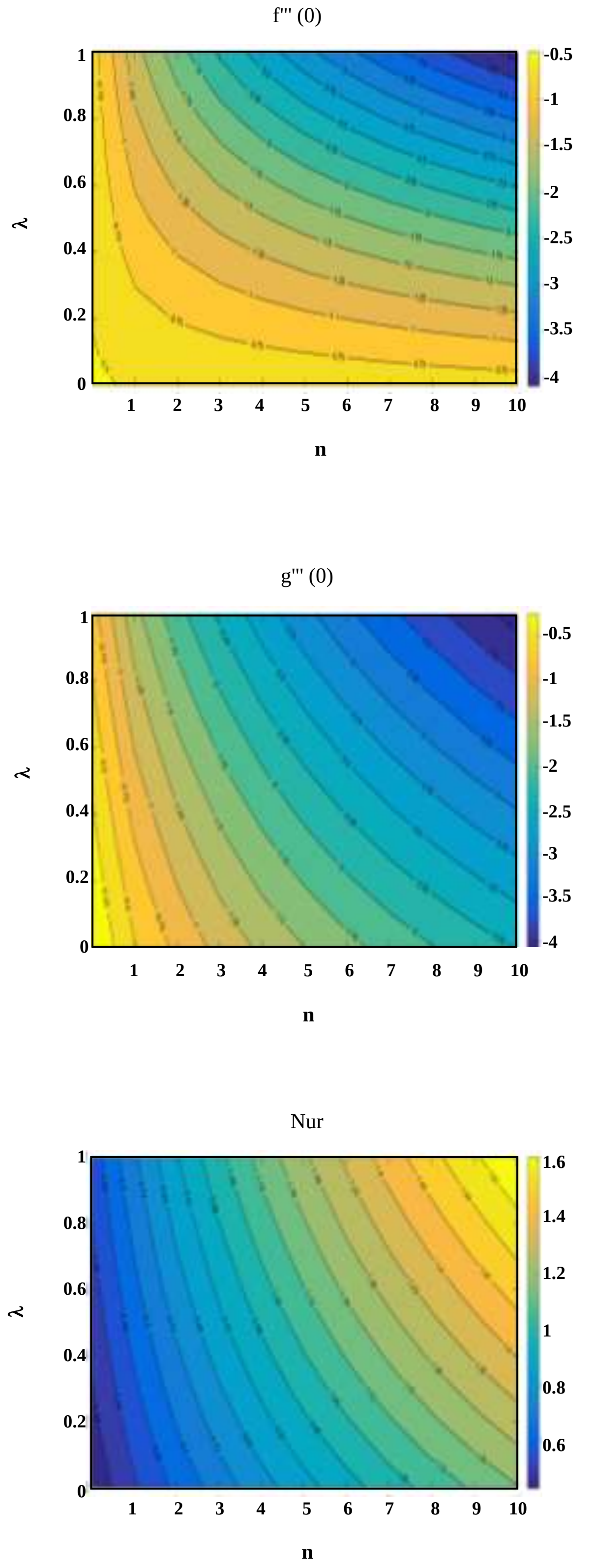

Fig. 10: Effect of n and λ on Nur, f"(0) and g"(0) when η_∞ = 7, Nb= 0.7, Nt= 0.4, Sc= 3, Pr= 1.

Received: May 23, 2017 ; Accepted : Dec. 12, 2017

REFERENCES

[1] Jing D., Hu Y., Liu M., Wei J., Guo L., Preparation of Highly Dispersed Nanofluid and CFD Study of Its Utilization in a Concentrating PV/T System, *Solar Energy* 112: 30–40 (2015).

[2] Gorji T.B., Ranjbar A. A., Geometry Optimization of a Nanofluid-Based Direct Absorption Solar Collector Using Response Surface Methodology, *Solar Energy* **122**: 314–325 (2015).

[3] Nasrin R., Alim M. A., Performance of Nanofluids on Heat Transfer in a Wavy Solar Collector, *International Journal of Engineering, Science and Technology*, **5**(3): 58-77 (2013).

[4] Junaid Ahmad Khan, Mustafa M., Hayat T., Alsaedi A., Three-Dimensional Flow of Nanofluid over a Non-Linearly Stretching Sheet: An Application to Solar Energy, *International Journal of Heat and Mass Transfer*, **86**: 158–164 (2015).

[5] Cregan V., Myers T.G., Modelling the Efficiency of a Nanofluid Direct Absorption Solar Collector, *International Journal of Heat and Mass Transfer*, **90**: 505–514 (2015).

[6] Turkyilmazoglu M., Performance of Direct Absorption Solar Collector with Nanofluid Mixture, *Energy Conversion and Management*, **114**: 1-10 (2016).

[7] Hatami M., Domairry G., Transient Vertically Motion of a Soluble Particle in a Newtonian Fluid Media, *Powder Technology*, **253**: 481-485 (2014).

[8] Hatami M., Ganji D.D., Motion of a Spherical Particle on a Rotating Parabola Using Lagrangian and High Accuracy Multi-Step Differential Transformation Method, *Powder Technology*, **258**: 94-98 (2014).

[9] Hatami M., Ganji D.D., Motion of a Spherical Particle in a Fluid Forced Vortex by DQM and DTM, *Particuology*, **16**: 206-212 (2014).

[10] Dogonchi A. S, Hatami M., Domairry G., Motion Analysis of a Spherical Solid Particle in Plane Couette Newtonian Fluid Flow, *Powder Technology*, **274**: 186-192 (2015).

[11] Haghshenas Fard M., Nasr Esfahany M., Talaie M.R., Numerical Study of Convective Heat Transfer of Nanofluids in a Circular Tube Two-Phase Model Versus Single-Phase Model, *International Communications in Heat and Mass Transfer*, **37**: 91-97 (2010).

[12] Göktepe S., Atalık K., Ertürk H., Comparison of Single and Two-Phase Models for Nanofluid Convection at the Entrance of a Uniformly Heated Tube, *International Journal of Thermal Sciences*, **80**: 83-92 (2014).

[13] Tauseef Mohyud-Din S., Zaidi Z. A., Khan U., Ahmed N., On Heat and Mass Transfer Analysis for the Flow of a Nanofluid between Rotating Parallel Plates, *Aerosp. Sci. Technol.* (2015).

[14] Hayat T., Imtiaz M., Alsaedi A, Kutbi M. A., MHD Three-Dimensional Flow of Nanofluid with Velocity Slip and Nonlinear Termal Radiation, *Journal of Magnetism and Magnetic Materials*, **396**: 31-37 (2015).

[15] Khan J.A., Mustafa M., Hayat T., Alsaedi A., Three-Dimensional Flow of Nanofluid over a Non-Linearly Stretching Sheet: An Application to Solar Energy, *Int. J. Heat. Mass. Trans.* **86**: 158-164 (2015).

[16] Shirvan K. M., Mamourian M., Mirzakhanlari S., Ellahi R., Vafai K., Numerical Investigation and Sensitivity Analysis of Effective Parameters on Combined Heat tTransfer Performance in a Porous Solar Cavity Receiver by rResponse Surface Methodology, *International Journal of Heat and Mass Transfer*, **105**: 811-825 (2017).

[17] Fakour M., Vahabzadeh A., Ganji D. D., Hatami M., Analytical Study of Micropolar Fluid Flow and Heat Tansfer in a Channel with Permeable Walls, *Journal of Molecular Liquids*, **204**: 198-204: (2015).

[18] Ghasemi S.E., Hatami M., Sarokolaie A.K., Ganji D.D., Study on Blood Flow Containing Nanoparticles Through Porous Arteries in Presence of Magnetic Field Using aAnalytical Methods, *Physica E: Low-Dimensional Systems and Nanostructures*, **70**: 146-156 (2015).

[19] Ghasemi S.E., Hatami M., Mehdizadeh Ahangar Gh.R., Ganji D.D., Electrohydrodynamic Flow Analysis in a Circular Cylindrical Conduit Using Least Square method, *Journal of Electrostatics*, **72** (1): 47-52 (2014).

[20] Rahimi-Gorji M., Pourmehran O., Hatami M., Ganji D.D., Statistical Optimization of Microchannel Heat Sink (MCHS) Geometry Cooled by Different Nanofluids Using RSM Analysis, *The European Physical Journal Plus*, **22**: 130, 1-21 (2015).

[21] Domairry, Hatami M., Squeezing Cu–Water Nanofluid Flow Analysis between Parallel Plates by DTM-Padé Method, *Journal of Molecular Liquids*, **193**: 37-44 (2014).

[22] Ahmadi A.R., Zahmatkesh A., Hatami M., Ganji D.D., A Comprehensive Analysis of the Flow and Heat Transfer for a Nanofluid Over an Unsteady Stretching Flat Plate, *Powder Technology*, **258**: 125-133 (2014).

[23] Hatami M., Ganji D.D., Thermal Behavior of Longitudinal Convective–Radiative Porous Fins with Different Section Shapes and Ceramic Materials (SiC and Si_3N_4), *Ceramics International*, **40**(5): 6765-6775 (2014).

[24] Hatami M., Ganji D.D., Investigation of Refrigeration Efficiency for Fully Wet Circular Porous Fins with Variable Sections by Combined Heat and Mass Transfer Analysis, *International Journal of Refrigeration*, **40**: 140-151 (2014).

[25] Hatami M., Mehdizadeh Ahangar GH.R., Ganji D.D., Boubaker K., Refrigeration Efficiency Analysis for Fully Wet Semi-Spherical Porous Fins, *Energy Conversion and Management*, **84**: 533-540 (2014).

[26] Hatami M., Mosayebidorcheh S., Jing D., Two-Phase Nanofluid Condensation and Heat Transfer Modeling Using Least Square Method (LSM) for Industrial Applications, *Heat and Mass Transfer* **53**(6): 2061-2072 (2017).

[27] Mosayebidorcheh S., Hatami M., Heat Transfer Analysis in Carbon Nanotube-Water between Rotating Disks under Thermal Radiation Conditions, *Journal of Molecular Liquids* (2017).

[28] Hatami M., Mosayebidorcheh S., Jing D., Thermal Performance Evaluation of Alumina-Water Nanofluid in an Inclined Direct Absorption Solar Collector (IDASC) Using Numerical Method, *Journal of Molecular Liquids*, **231**: 632-639 (2017).

[29] Mosayebidorcheh S., Tahavori M. A., Mosayebidorcheh T., Ganji D. D., Analysis of Nano-Bioconvection Flow Containing Both Nanoparticles and Gyrotactic Microorganisms in a Horizontal Channel Using Modified Least Square Method (MLSM), *Journal of Molecular Liquids*, **227**: 356-365 (2017).

[30] Hatami M., Mosayebidorcheh S., Geng J, Jing D., Heat Transfer and Nanofluids Flow Through the Circular Concentric Heat Pipes: a Comparative Study Using Least Square Method (LSM), *Journal of Mathematics and computer Science-JMCS*, **17** (2): 235-245 (2017).

[31] Mosayebidorcheh S., Sheikholeslami M., Hatami M., Ganji D.D., Analysis of Turbulent MHD Couette Nanofluid Flow and Heat Transfer Using Hybrid DTM–FDM, *Particuology* **26**: 95-101 (2016).

[32] Keller H. B., "A New Difference Scheme for Parabolic Problems, Num. Solns. of Partial Differential Equations", II (Hubbard, B. ed.)., 327-350. New York: Academic Press, 1971.

[33] Bradshaw P., Cebeci T., Whitelaw J. H., "Engineering Calculation Methods for Turbulent Flow", Academic Press, (1981).